Relaxation phenomenon after changing lanes: an experimental validation with the NGSIM dataset

Ludovic LECLERCQ
Nicolas CHIABAUT
Jorge LAVAL
Christine BUISSON

Laboratoire Ingénierie Circulation Transport LICIT (ENTPE / INRETS)
Rue Maurice Audin
F 69518 Vaulx-en-Velin
Tel: +33 4 72 04 77 16
Fax: +33 4 72 04 77 12
Email: leclercq@entpe.fr

Paper submitted for presentation and publication to the 86th meeting of the *Transportation Research Board*
Submission date: 1st August 2006
3668 Words + 7 figures = 5418 words

Abstract

This paper presents a calibration and analysis of a relaxation model recently proposed which requires only one additional parameter ε. The relaxation phenomenon takes place whenever a lane change occurs at a short spacing that falls outside the fundamental diagram. Such non-equilibrium spacing poses problems to car-following rules that can only handle equilibrium ones. The relaxation model has been already calibrated with macroscopic data. This paper uses trajectory data from NGSIM to undertake a more rigorous calibration and validation. It is found that for a given driver there exists a value of ε that reproduces the relaxation process with uncanny accuracy and that the mean ε value does not worsen the fit significantly.

1. INTRODUCTION

The relaxation phenomenon (*1-2*) takes place when the lane-changing vehicle imposes short (non-equilibrium) spacings immediately after the lane change with its leader and/or its follower on the target lane. Smith (*3*) observed that vehicles involved in a lane-changing maneuver accept short spacings during the first 20 or 30 seconds, gradually attaining more comfortable spacings.

In situation of short spacings, car-following rules based on a fundamental diagram (FD) predict speeds far below empirical observations (we call this the "*overreaction effect*"). Furthermore, the predicted speed can be negative if the spacing is less than the jam spacing. This poses great difficulties in the implementation of lane-changing in microscopic models. In particular, gap-acceptance models induce too few lane changes since they do not capture the relaxation phenomenon. The common solution has been to incorporate forced and cooperative lane-changing procedures that introduce numerous additional parameters which are difficult to calibrate (*4-8*).

To the authors' knowledge only one publication proposes a formulation for the representation of relaxation inside microscopic models (*2*). In this reference the non-equilibrium spacing is relaxed linearly to the equilibrium value within a fixed time interval. Unfortunately, the same car-following rule is used with this modified spacing which leads to overreaction effect.

Recently Laval and Leclercq (*9*) have proposed the microscopic formulation of the macroscopic multilane hybrid model in (*10*), which shows that most traffic instabilities are due to lane-changing (*11-12*). This microscopic formulation incorporates a relaxation procedure with only one additional parameter, ε, and has been validated at a macroscopic level (lane-changing rate, capacity drop, bottleneck discharge rate).

The aim of this paper is to validate the relaxation model proposed in (*9*) at a microscopic scale using the NGSIM vehicle trajectory dataset (*13*). It is found that this model fits extremely well the trajectory of vehicles during the relaxation phase provided that ε is calibrated for each vehicle. Moreover, if the mean value of ε is used for all vehicles, the overall fit is only slightly deteriorated.

This paper is organized as follows: section 2 provides some background on the relaxation model in (*9*); section 3 presents the relaxation phenomenon at the macroscopic scale of the FD; section 4 is devoted to the calibration and the validation of the relaxation model at a microscopic level. Finally, section 5 presents a brief discussion.

2. BACKGROUND: THE RELAXATION MODEL

Consider the diagram in Figure 1, which shows the trajectory of the three vehicles involved in a lane change maneuver. The lane-changing vehicle (*c* in the figure) cuts-in between the leader (*l*) and the follower (*f*) vehicles in the target lane at time t_0. At this time the spacing of the follower changes from $s_f(t_0^-)$ to $s_f(t_0^+)$ as its new leader becomes *c*, which sees a spacing of $s_c(t_0^+)$ in front of him. When $s_f(t_0^+)$ and/or $s_c(t_0^+)$ are non-equilibrium values (i.e., a spacing less than the FD-spacing associated to the leader speed) the relaxation procedure starts.

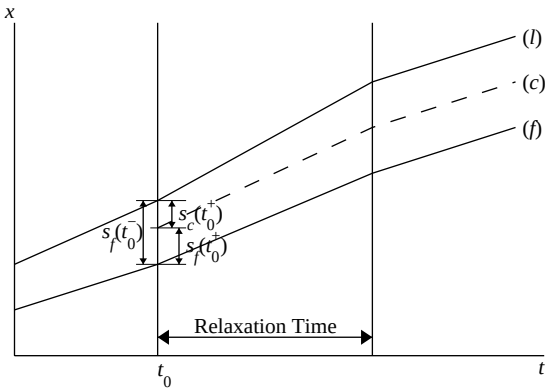

Figure 1: Space-time diagram

It was shown in (*10*) that the effect of lane-changing can be captured accurately when considered the changer as a moving bottleneck (*14-15*). In this spirit the model in (*9*) considers lane changers that are in non-equilibrium as

moving bottlenecks, which amounts to introduce moving boundary conditions on the target lane in the car-following framework. It was shown in (*9*) that this can be accomplished using an extension to Newell's simplified car-following model (*16*):

$$x_i^{t+\Delta t} = \min\left(\underbrace{x_i^t + \min(u, v_i^t + a\Delta t)\Delta t}_{\text{free-flow term}} ; \underbrace{x_{i-1}^{t+\Delta t} + v_{i-1}^{t+\Delta t}\Delta t - \frac{\Delta N_i^{t+\Delta t}}{K(v_{i-1}^{t+\Delta t})}}_{\text{congested term}} \right) \quad (1)$$

where ΔN_i^t is the difference in vehicle number between two consecutive vehicles i and i-1 at time t, x_i^t and v_i^t are the position and velocity of vehicle i at time t, Δt is the time-step, u the free-flow speed, a the maximum acceleration and $K(v)$ gives the density in congestion associated with speed v for a triangular FD: i.e.,

$$K(v) = \frac{w\kappa}{w+v} \quad (2)$$

where w is the wave-speed and κ the jam density.

In the relaxation phase (when the vehicle is considered as a boundary condition and not as a particle) ΔN_i is lower than 1. At the beginning of this phase is determined by the ratio between the spacing at the moment at the lane-change over the FD-spacing associated to the leader speed. The time evolution of ΔN_i is given by:

$$\Delta N_i^{t+\Delta t} = \min\left(1, \Delta N_i^t \left(\frac{1}{K(v_i^t)} + (v_i^{t+\Delta t} - v_i^t + \varepsilon)\Delta t \right) K\left(v_i^{t+\Delta t}\right) \right) \quad (3)$$

The parameter ε in (3) can be interpreted as the difference in speed the lane-changer is willing to maintain with its leader in order to attain an equilibrium spacing.

Note that during the relaxation phase the congested term in (1) is predominant. This phase ends when ΔN_i^t reaches one. At this moment the changer is no longer a moving boundary condition but an actual vehicle. Finally, note that $\Delta t = 1/w\kappa$, which ensures that the numerical scheme is exact when the FD is triangular.

3. RELAXATION PHENOMENON AT THE MACROSCOPIC SCALE

3.1. Relaxation to equilibrium

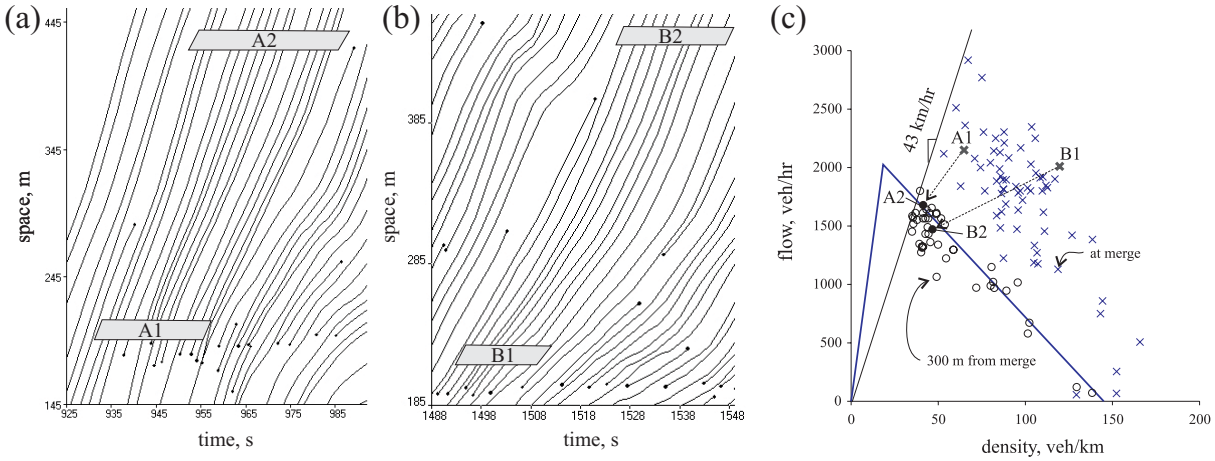

Figure 2: Relaxation to equilibrium. (a)-(b) Vehicle trajectories in the shoulder lane (c) Flow-density measurements in this lane immediately downstream (crosses) and 300 m downstream (circles) of the on-ramp.

Figures 2a-b show two sets of trajectories taken from the NGSIM dataset for the shoulder lane in the vicinity of Powell St on-ramp on I-80 freeway in Berkeley, California. It can be seen how small spacings are accepted near the on-ramp, followed by a gradual relaxation into more comfortable values. Part c of the figure shows flow-density measurements in this lane immediately downstream of the on-ramp (crosses) and 300 m downstream (circles). These measurements were calculated using Edie's method (*17*) for numerous regions similar to the shaded regions in parts a and b of the figure. These regions were chosen so that the same vehicles are measured

at both locations. It can be seen that measurements near the on-ramp are in non-equilibrium, but converge to stable values further downstream after approximately 30 seconds. These values define the congested branch of a triangular FD with w=15 km/hr and κ=150 veh/km.

Notice that in the NGSIM dataset only congestion traffic states are observed. The maximum observed mean speed is 43 km/hr in the shoulder lane as shown in Figure 2c. Although this dataset does not cover all the possible traffic states, it still provides a valuable source for model validation.

3.2. Relaxation paths in the FD

In this subsection we study the paths of (q,k) measurements in the FD during the relaxation phase; e.g., the paths from A1 to A2 in Figure 2c. This is done by measuring the flow q and the density k at consecutive locations following the same group of vehicles; see Figure 3a. The results are shown in Figure 3b. Two sets of similar paths can be identified in this figure: a "vertical" and a "horizontal" set.
It turns out that these sets can be explained analytically with the relaxation model on the previous section. Indeed, it has been proven in (*9*) that the continuum formulation of (3) for the case of a constant leader acceleration, β, starting at a speed v_0, is given by:

$$s(t) = \left(1 + c_1 t\right)\left(s(0) + \frac{\varepsilon}{c_1} \ln\left(1 + c_1 t\right) \right) \tag{4}$$

where $c_1=\beta/(v_0+w)$. This gives $k(t)=1/s(t)$. To obtain $q(t)$, we note that:

$$q(t) = \left(v_0 + \beta t\right) k(t) \tag{5}$$

The system of equations (4)-(5) defines the family of relaxation paths in the FD in parametric form, with initial conditions v_0 and β and for a given ε. Figure 3c shows some realizations of this system for several values of v_0 and β and ε=2.2 km/hr, which corresponds to the mean value observed in our sample (see section 4). It can be seen that the sets of path predicted by this system are consistent with the observed paths.

This result is reassuring because it indicates that the model is well defined and produces reasonable predictions. However, this is not sufficient to validate the relaxation model. In the next section, we study the prediction of the model for individual vehicles trajectories.

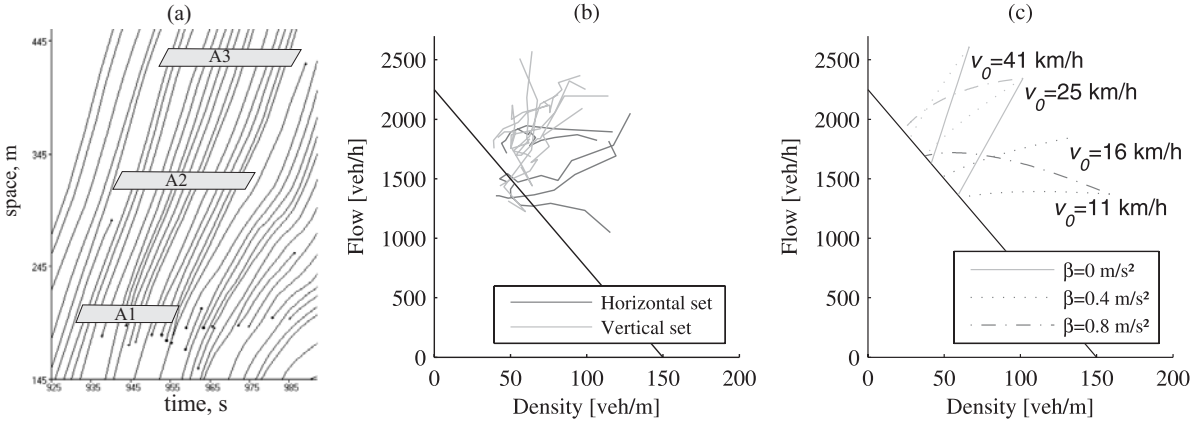

Figure 3: Relaxation paths. (a) Vehicle trajectories in the shoulder lane (b) Measured paths (c) Predicted paths

CALIBRATION AND ANALYSIS OF THE RELAXATION MODEL AT THE MICROSCOPIC SCALE

In this section we use the trajectories from the NGSIM dataset for calibrating and analyzing the relaxation model. This was done in three steps. First, a filtering of the database is undertaken in order to select consecutive pair of trajectories where relaxation occurs after lane-changing. Second, ε is calibrated for every vehicle pair. Third, the model is tested by comparing its performance with ε given by its mean. Additionally, it is compared to the car-following model without relaxation.

Filtering

The first stage of the filtering process consisted in identifying "stable lane changes". A pair of trajectories is defined as "stable" if the two vehicles involved stay in the target lane during a time T, long enough for the relaxation phenomenon could occur. If T is to short the relaxation procedure is not observed completely; if it is too large chances are that one of the vehicles will change lane and therefore be not considered. A good compromise seems to be T=20 s, which results in 1539 pairs of stable trajectories.

The second stage of the filtering consisted in identifying lane-changes that induce non-equilibrium spacings. We say that a spacing s is in non-equilibrium if

$$s < 0.8 s_0 \tag{6}$$

where s_0 is the FD-spacing associated to the leader speed v_0 at the beginning of the relaxation period t_0.

$$s_0 = \frac{w + v_0}{w\kappa} \tag{7}$$

Notice that t_0 may differ from the time of the lane changing, t_c, reported in the NGSIM dataset. Indeed this time refers to instant where the lane-changer crosses the lane separation line and not to the instant where the vehicle is completely in the target lane. We define t_0 has the instant where the spacing is minimum after t_c. The values of w and κ have been calibrated in the previous section. The factor 0.8 in (6) appears to be a reasonable value to ensure that relaxation takes place indeed; i.e. it ensures that the initial spacing is small enough with respect to the FD-spacing. Note that non-equilibrium spacings may take place between the lane changer and its leader and/or between the follower and the lane-changer; see Figure 1. As a result, 1094 vehicle pairs correspond to stable and non-equilibrium lane changes.

Finally, Figure 4 presents the summary of the filtering process. For each target lane, the total number of lane changers, the number of stable lane changes and the number of lane changes satisfying (6) are shown in Figure 4b for each origin lane. It can be seen that most non-equilibrium lane changes come from lanes 5, 6 and 7, which is not surprising since they constitute a weaving section.

The pairs of trajectories resulting from the filtering process described in this section define a set, S, where ε will be calibrated.

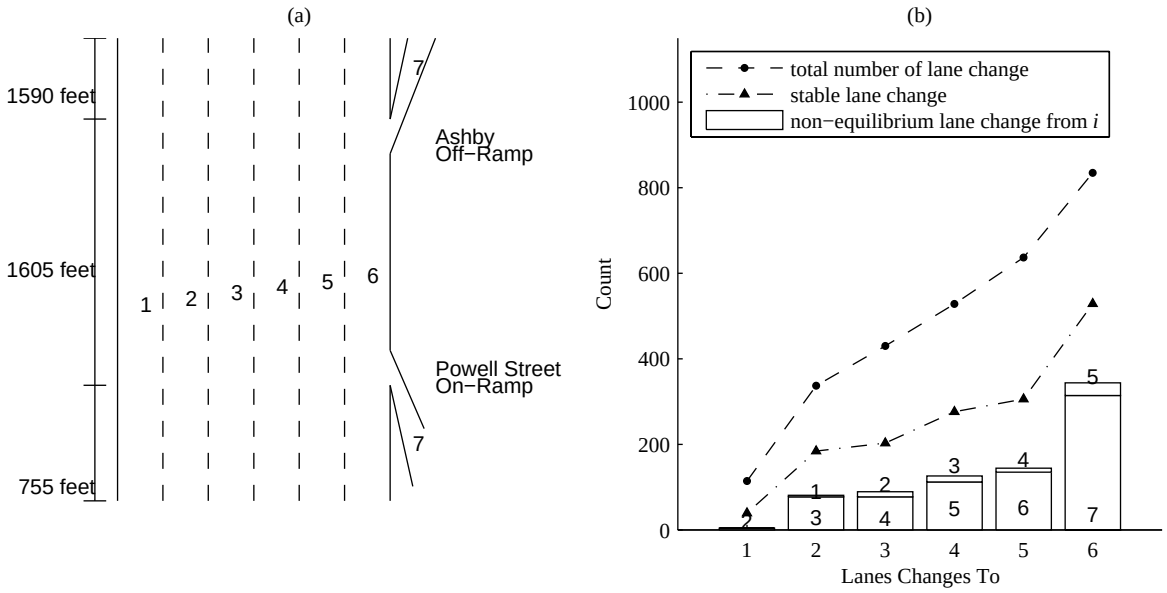

Figure 4: Filtering process. (a) Site description (b) Total number of lane changers and the number of lane changes satisfying (6) for each origin lane

Calibration of ε for each vehicle pair

Consider the following "lead-vehicle problem" (LVP) with the following initial and boundary data: (i) the trajectory of the lead vehicle, and (ii) the initial position of the following car. The trajectory of the following car

is computed using (1) for all $\varepsilon \in [-\varepsilon_{max}, \varepsilon_{max}]$. Note that since the initial spacing between the two vehicles is always lower than the equilibrium spacing, (1) reduces to its congested term.

The previous LVP is solved for each pair i of vehicle in S considering n time-steps Δt. Optimal ε-value for pair i, ε_i^*, minimizes the sum of square between the computed solution and the experimental data (SSE). This procedure is applied with ε_{max}=8 m/s, n=12 and $\Delta t = 1/w\kappa$=1.6 s. The ε-values are tested with a step $\Delta\varepsilon$ equal to 0.05 m/s.

Figure 5 presents a couple of typical LVP solutions, which shows the remarkable agreement between the model and the data. This is a especially appealing result since it suggests that a single parameter is able to capture the complexity of the relaxation phenomenon. Indeed 988 vehicle pairs in S (90%) exhibit a root mean squared error RMSE less than 4 m ($RMSE = \sqrt{SSE/n}$). A visual inspection of a sample of trajectories with RMSE greater than 4 m revealed measurement errors: sudden stop of the leader, errors in the estimation of t_0 due to errors in the reported value of t_c, sudden discontinuities in the acceleration profiles certainly due to errors in the position of the vehicle. We decide to eliminate this subset from S. Let S' be the resulting set of vehicle pairs.

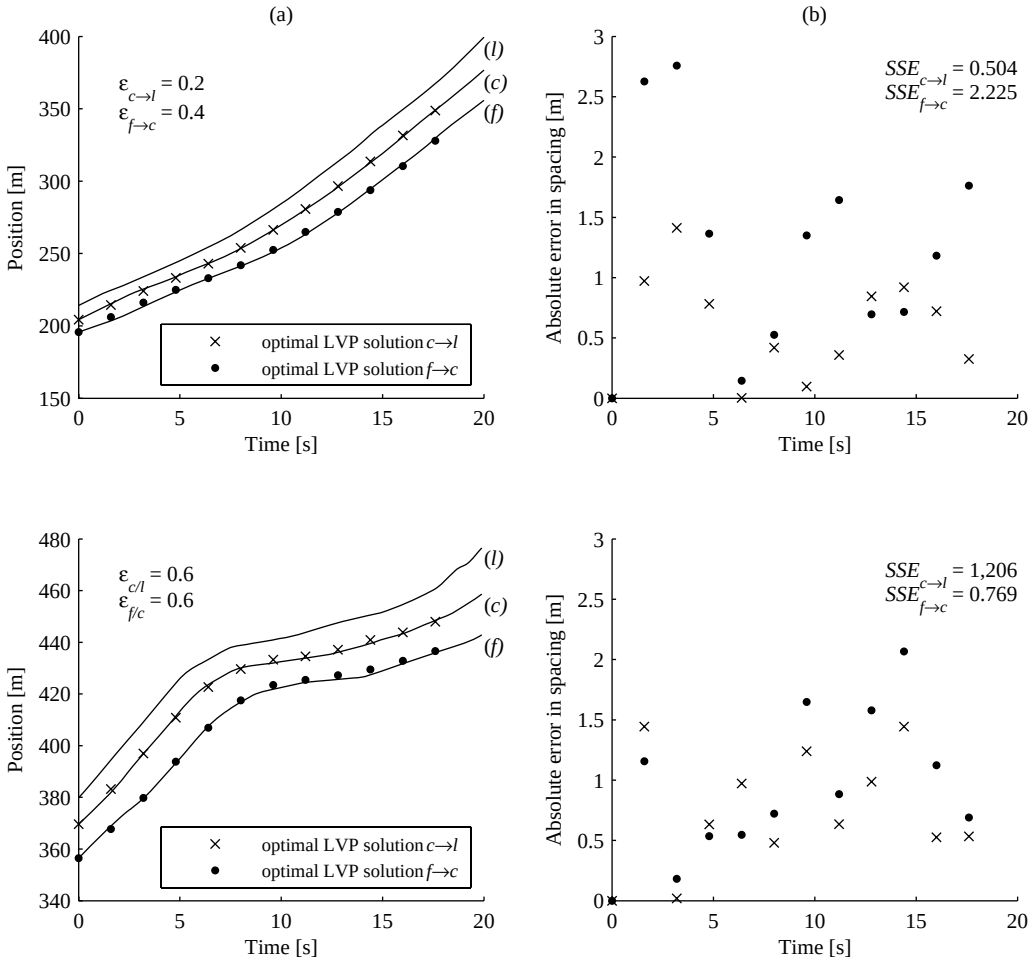

Figure 5: LVP solutions for two typical cases. (a) Time-space diagram (b) Errors in spacing between the computed solution and the experimental data

The distribution of the results is presented in Figure 6. Part a of the figure shows the histogram for S', where it can be seen that approximately 22 trajectories (2.2%) exhibit ε^* less than or equal to 0. These cases correspond to aggressive drivers since they tend to continuously reduce their spacing up to a point where they stabilize it at a non-equilibrium value. These "contractions" constitute a different phenomenon and should be considered

separately from the relaxation model calibration. It can also be seen on the figure that approximately 21 cases (2.1%) may be considered as outliers ($\varepsilon^* > 10$ km/h). Both these cases will be eliminated from our sample in the sequel. Let *S''* be the (final) resulting sample.

Figure 6b shows the histogram corresponding to *S''*. The parameters of the distribution of ε^* are $\overline{\varepsilon}$ =2.2 km/hr and σ=1.8 km/hr. Notice that the index of dispersion ($\sigma / \overline{\varepsilon}$) is low (equal to 0.8), which indicates that most of the values are close to the mean. Figure 6c presents the confidence intervals (with a level of certainty α=0.95) of $\overline{\varepsilon}$ for each target lane. Note that lane 1 is the target for 4 lane changes only, which is not sufficient to define a $\overline{\varepsilon}$ for this lane. On lane 6 $\overline{\varepsilon}$ is statistically lower than on the other lanes. This is not surprising as lane 6 is the shoulder lane where drivers have to be more aggressive to enter or to leave the highway. Therefore, one may conjecture that using two values for $\overline{\varepsilon}$, one for vehicles on lane 6 $\overline{\varepsilon}_6$ =1.8 km/h and the other $\overline{\varepsilon}_{2\to5}$ =2.5 km/h for vehicles on lanes 2 to 5 would provide a good overall fit for the relaxation model. In fact, in the next section we verify this.

Finally, Figure 6d establishes that we can not reject the hypothesis that the relative position (lane changer or follower) play no role in the relaxation process; i.e., $\overline{\varepsilon}$ remains within the confidence intervals computed for follower and lane changer trajectories.

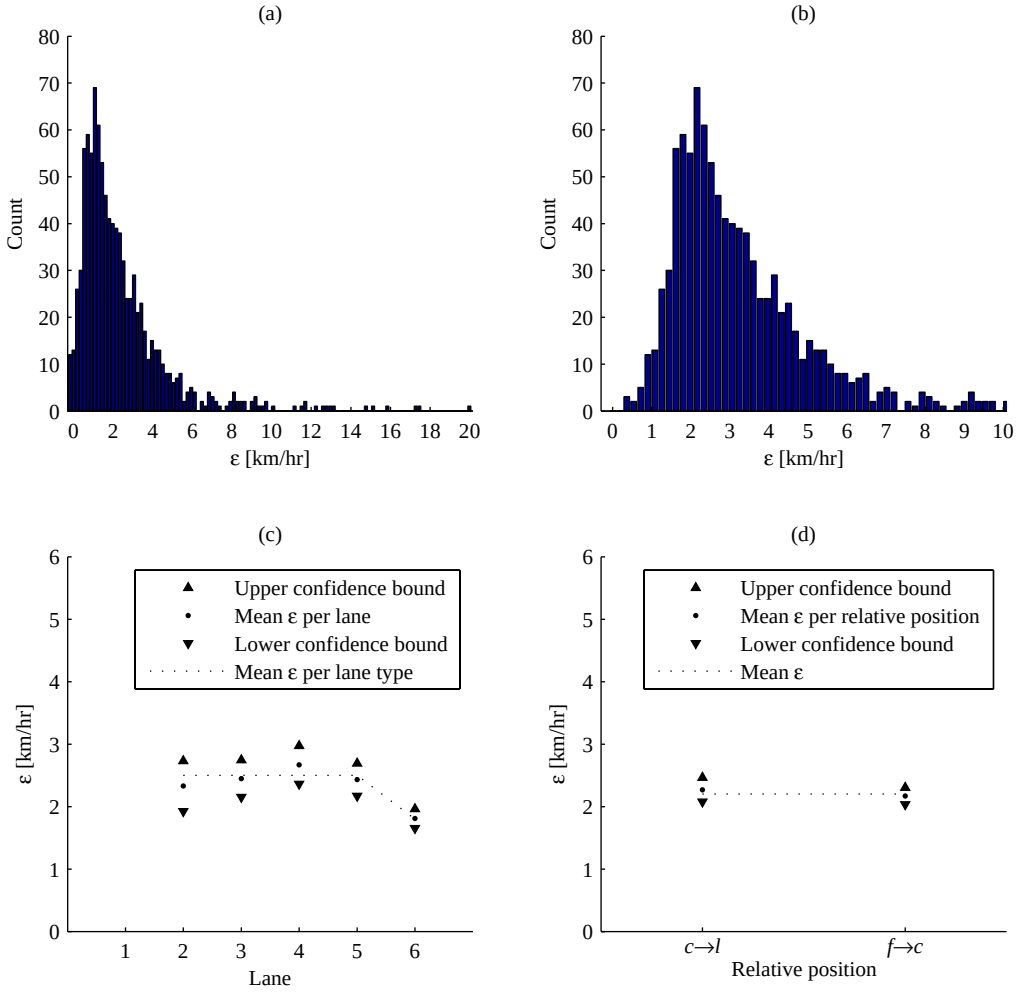

Figure 6: Statistical analysis of results. (a) Histogram for *S'* (b) Histogram for *S''* (c) Confidence intervals across lanes (d) Confidence intervals for follower and lane changer

Model analysis

Here we test the relaxation model by comparing the RMSE obtained with (i) the optimal value of ε for each pair of trajectories; (ii) an ε value equal to $\bar{\varepsilon}$ for all trajectories pair; and (iii) no relaxation (i.e. ΔN_i is set to 1 in (3) for all t). The results are presented in Figure 7a, which shows the RMSE of a subset of *S''* (corresponding to ε^* values equal to 1.1, 1.3 and 1.5 km/h) for cases (i), (ii) and (iii). The complete set contains 945 vehicle pairs and cannot be fully displayed. As conjectured in the previous subsection, the use of $\bar{\varepsilon}$ instead of ε^* only slightly degrades the fit. In fact, the mean RMSE for *S''* is equal to 1.5 m with ε^* and to 2.5 m with $\bar{\varepsilon}$; i.e., a difference of only 1 m. As expected, case (iii) leads to a marked increase in RMSE with a mean equal to 4.0 m. This result highlights the existence of a relaxation phase that must not be ignored.

Figure 7b shows the cumulative distribution of RMSE for the three cases under consideration, which reinforces previous conclusions. Indeed, take the example of 80% percentile: in this case the RMSE for case (i) is 1.9 m, which only deteriorates to 3.4 m for case (ii) and jumps to 5.5 m for case (iii). Note too that only 48% of the set *S''* has a RMSE lower that 3.4 m in case (iii).

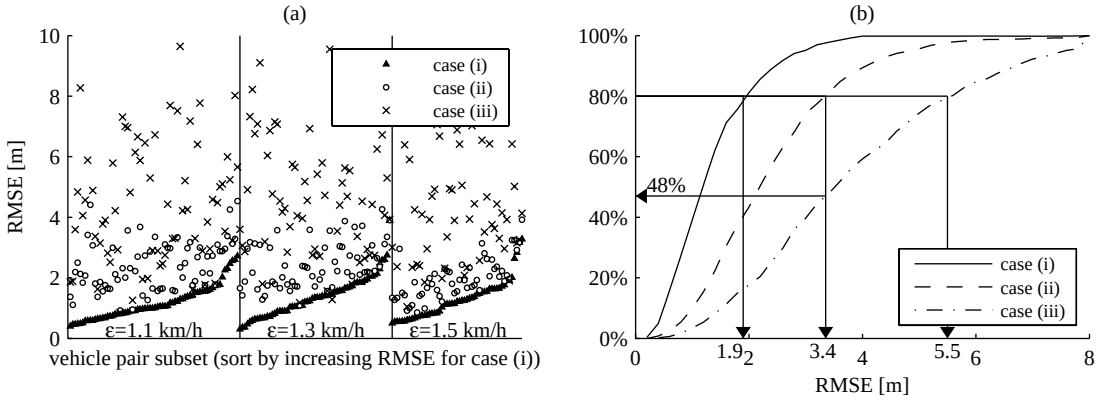

Figure 7: Validation results. (a) RMSE for each pair of vehicles in set *S''* (b) cumulative distribution of RMSE

DISCUSSION

It is encouraging that a single parameter is able to capture most the complexity involved in the relaxation process. Unfortunately, this parameter is not readily observable in the field. However, since it has a clear physical meaning it can be calibrated separately from the rest of the car-following parameters. One can calibrate ε using the method of this paper, which works for arbitrary lead-vehicle trajectories. Another possibility is fitting (4) when the leader acceleration is constant during all the relaxation process. This method is of limited interest because it is difficult to find lead-vehicle trajectories with constant acceleration for a long enough periods of time. But this method could be of interest in the context of field experiment, where one has control of the leader's trajectory.

It is worth noting that in this paper the measure of error considered only two consecutive vehicles; i.e., error propagations were not studied. Note that the car-following rule (1) is a contraction mapping in equilibrium (ΔN_i=1); see (*18*). This means that the errors generated at the source (lane-changing) would not grow in time, provided that (i) upstream traffic is in equilibrium and (ii) there are no lane changes upstream. When (i) and (ii) are satisfied the error generated by an inappropriate representation of the relaxation between two vehicles is confined to a finite region in time-space; i.e. for a given vehicle upstream of the lane change the error will be noticeable only inside that region. However, (i) and (ii) are never satisfied in practice. Furthermore, a model without relaxation will produce stoppage waves that will propagate upstream indefinitely in congestion. This could induce additional errors such as extra lane changes, lower entry flow from on-ramps, etc. Given the complexity involved, this error can only be quantified using simulation.

Finally, this paper has identified aggressive vehicles for which the spacing decreases after the lane change. Interestingly, the relaxation model (1) with negative ε also gives good fit in this case. However, since aggressiveness corresponds to a different driver behavior, negative ε values must not be incorporate in the mean

value used for relaxation. One should incorporate aggressiveness by introducing the proportion of drivers that are aggressive and estimate a separate (negative) ε value. This is being investigated by the authors.

REFERENCES

1. Wei, C., Meyer, E., Lee, J., Feng, C. Characterizing and modeling observed lane-changing behavior: lane-vehicle-based microscopic simulation on urban street network. *Transportation Research Record* n°1710. TRB National Research Council: Washington, D.C., 2000, 104-113.
2. Cohen, S.L. Application of relaxation procedure for lane changing in microscopic simulation models. Transportation Research Record n°1883. TRB National Research Council: Washington, D.C., 2004, 50-58.
3. Smith, S.A. *Freeway data collection for studying vehicle interaction*. Tech. Rep. FHWA/RD-85/108, FHWA, U.S., Department of Transportation, 1985.
4. Gipps, P. G. Multsim: a model for simulating vehicular traffic on multi-lane arterial roads. *Mathematics and Computers in Simulation*, 28(4), 1986, 331 295.
5. Hidas, P. Modelling lane changing and merging in microscopic traffic simulation. *Transportation Research Part C*, 10(5-6), 2002, 351-371.
6. Hidas, P. Modelling vehicle interactions in microscopic simulation of merging and weaving. *Transportation Research Part C*, 13(1), 2005, 37-62.
7. Wagner, P., Nagel, K., Wolf, D. Realistic multi-lane traffic rules for cellular automata. *Physica A*, 234(3-4), 1997, 687-698.
8. Ahmed, K., Ben-akiva, M., Koutsopoulos, H., Mishalani, R. Models of freeway lane changing and gap acceptance behavior. In: Lesort, J. B. (Ed.), *13th Int. Symp. on Transportation and Traffic Theory*. Elsevier, New York, 1996.
9. Laval, J.A., Leclercq, L. A microscopic theory of lane-changing. *Submitted for publication*, 2006. Avalaible as Research Report LICIT 06-04, Institut National de Recherche sur les Transports et leur Sécurité (INRETS), Bron, France.
10. Laval, J.A., Daganzo, C. F. Lane-changing in traffic streams. *Transportation Research B*, 40(3), 2006, 251-264.
11. Laval, J.A., Cassidy, M.J., Daganzo, C.F. Impacts of lane changes at on-ramp bottlenecks: a theory and strategies to maximize capacity. In: Kühne, R., Poschel, T., Schadschneider, A., Schreckenberg, M., Wolf, D. (Eds.), *Traffic and Granular Flow'05*. Springer, 2005.
12. Laval, J.A. Linking synchronized fow and kinematic wave theory. In: Kühne, R., Poschel, T., Schadschneider, A., Schreckenberg, M., Wolf, D. (Eds.), *Traffic and Granular Flow'05*. Springer, 2005.
13. NGSIM. Next generation simulation. URL: http://ngsim.fhwa.dot.gov/, 2006.
14. Newell, G.F. A moving bottleneck. *Transportation Research B*, 32(8), 1998, 531–537.
15. Leclercq, L. Chanut, S., Lesort, J.B. Moving bottlenecks in the LWR model: a unified theory. *Transportation Research Record* n 1883. TRB National Research Council: Washington, D.C., 2004, 3–13.
16. Newell, G.F. A simplified car-following theory: a low-order model. *Transportation Research B*, 36(3), 2002, 195-205.
17. Edie, L. C. Car following and steady-state theory for non-congested traffic. Operations Research, 9, 1961, 66-77.
18. Daganzo, C.F. In Traffic Flow, Cellular Automata = Kinematic Waves. *Transportation Research part B*, 40(5), 2006, 396-403.